

# Measurement of the Schottky barrier height between Ni-InGaAs alloy and In<sub>0.53</sub>Ga<sub>0.47</sub>As

Shlomo Mehari,<sup>1,a)</sup> Arkady Gavrilov,<sup>1</sup> Shimon Cohen,<sup>1</sup> Pini Shekhter,<sup>2</sup> Moshe Eizenberg,<sup>2</sup> and Dan Ritter<sup>1</sup>

<sup>1</sup>Department of Electrical Engineering, Technion-Israel Institute of Technology, Haifa 32000, Israel

<sup>2</sup>Department of Materials Engineering, Technion-Israel Institute of Technology, Haifa 32000, Israel

(Received 28 June 2012; accepted 30 July 2012; published online 14 August 2012)

The temperature dependence of the current-voltage characteristics of Ni-InGaAs alloy Schottky contacts to n-In<sub>0.53</sub>Ga<sub>0.47</sub>As was measured. Nearly ideal plots with an ideality factor close to unity were obtained. The Arrhenius curve across the wide temperature range of 80–300 K was perfectly linear, yielding a barrier height of  $0.239 \pm 0.01$  eV. This value is substantially larger than previously reported. Conventional metal based Schottky diodes did not exhibit an ideal Schottky behavior. The ideal Schottky diode characteristics are attributed to the lack of oxidation and contamination of the interface between Ni-InGaAs and InGaAs. © 2012 American Institute of Physics. [<http://dx.doi.org/10.1063/1.4746254>]

Compound semiconductors and, in particular, In<sub>0.53</sub>Ga<sub>0.47</sub>As, are intensively studied as an alternative channel material for future metal-oxide-semiconductor field effect transistors. One of the many challenges to be overcome is the reduction of the series resistance to the source and drain. Recently, “silicide-like” Ni-InGaAs alloyed contacts to the InGaAs channel were introduced as a self-aligned metallization method and an alternative to ion implantation of the drain and source.<sup>1–3</sup> The series resistance obtained by this technology critically depends on the barrier height between the Ni-InGaAs alloy and InGaAs. Ivana *et al.*<sup>2</sup> evaluated the Schottky barrier height (SBH) between Ni-InGaAs and p-type InGaAs by photoelectron spectroscopy and obtained a value of  $0.8 \pm 0.1$  eV at room temperature. They concluded that the electron SBH is negative ( $-0.06$  eV). Kim *et al.*<sup>3</sup> reported that the electron SBH obtained from the temperature dependence of the I-V curves is 0.12 eV, but the details of the experiment and measured I-V curves were not described. In this letter, we report on detailed measurements of the temperature dependence of Ni-InGaAs/n-In<sub>0.53</sub>Ga<sub>0.47</sub>As Schottky diode I-V curves. A nearly ideal behavior was obtained, indicating that the interface between Ni-InGaAs and InGaAs was clean and oxide free, as expected for silicide-like contacts. The Arrhenius plot across the entire temperature range of 80–300 K was linear, and as a result an accurate evaluation of SBH was obtained. The extracted barrier height was  $0.239 \pm 0.01$  eV, a considerably larger value than reported before. Conventional metal based diodes were studied for reference purposes and found to exhibit much less ideal I-V curves.

We define an ideal Schottky diode as a junction having an ideal metal semiconductor interface, with a current voltage relationship given by<sup>4</sup>

$$I = I_0 \exp\left(\frac{q(V - IR_S)}{nk_B T}\right) \left(1 - \exp\left(-\frac{qV}{k_B T}\right)\right), \quad (1)$$

where  $V$  is the applied voltage,  $k_B$  is Boltzmann’s constant,  $T$  the absolute temperature,  $R_S$  the serial resistance, and  $q$  the electron charge. The ideality factor,  $n$ , is determined by image force barrier lowering and thermionic assisted tunneling and depends on the doping level and barrier height.<sup>4</sup> Its theoretical value is of the order of 1.02 for the diodes we have studied. The saturation current  $I_0$  is given by

$$I_0 = AA^{**}T^2 \exp\left(-\frac{q\phi_B}{k_B T}\right), \quad (2)$$

where  $A$  is the contact area,  $A^{**}$  the effective Richardson constant, and  $\phi_B$  is the Schottky barrier height. Neglecting the voltage drop across the serial resistance one obtains from Eq. (1) that<sup>4</sup>

$$\ln[I/\{1 - \exp(-qV/k_B T)\}] = \ln(I_0) + \frac{qV}{nk_B T}. \quad (3)$$

Equation (3) indicates that in the ideal case the ideality factor and saturation current can be obtained from any voltage range at either forward or reverse bias. In practice, however, most Schottky diodes are not ideal, and experimental plots of the left hand side of Eq. (3) as a function of the voltage are linear only across a limited voltage range. Non-ideal behavior of Schottky diodes may be due to interface states within a thin oxide layer between the metal and the semiconductor, generation-recombination currents within the space charge region, and interface or barrier height inhomogeneity.<sup>5–7</sup>

To create the Ni-InGaAs alloy 6 nm of Ni were deposited by electron beam evaporation on a 200 nm thick InGaAs layer. The wafer was annealed in forming gas atmosphere at a temperature of 250 °C for 1 min by rapid thermal annealing. The ramp up rate was 2 °C/s. The HRTEM cross section micrograph of the film shown in Fig. 1(b) indicates that the interface between the alloy and InGaAs is fairly abrupt. The nickel concentration in the layer was uniform, as verified by a secondary ion mass spectroscopy (SIMS) depth profile. The 2θ x-ray diffraction (XRD) patterns of bare InGaAs and InGaAs with deposited Ni before and after RTA were

<sup>a)</sup>Electronic mail: smehari@tx.technion.ac.il.

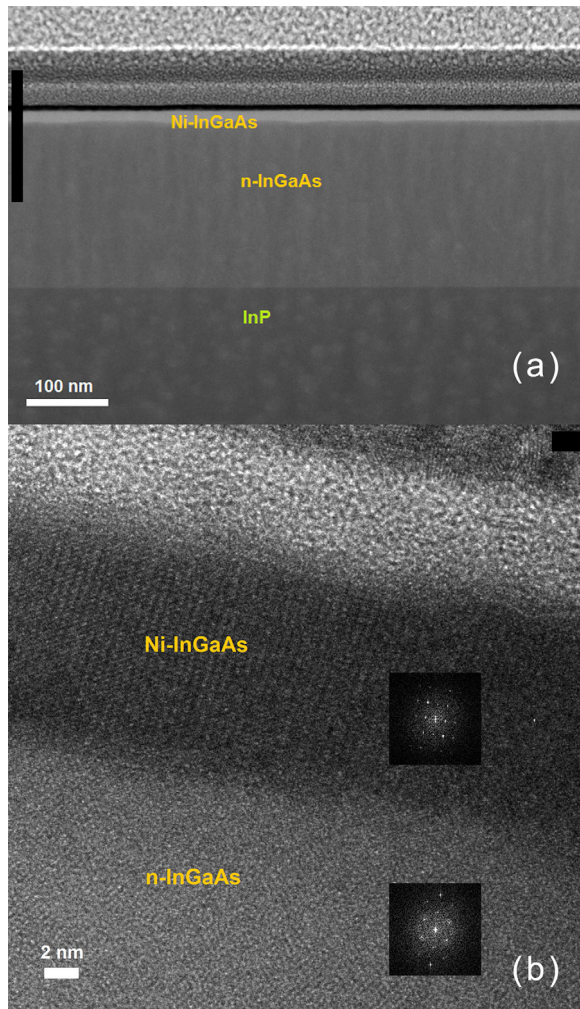


FIG. 1. (a) HAADF-STEM micrograph of Ni-InGaAs layer prepared by evaporation of 6 nm thick Ni on a 200 nm thick InGaAs layer, followed by rapid thermal annealing at 250 °C for 1 min showing the interfaces on a large scale. (b) HRTEM cross section micrograph (the insets show the diffraction patterns of the lattice as computed by fast Fourier transform). The zone axis is 40° of the InGaAs lattice.

obtained using Rigaku Smart Lab x-ray diffractometer with Cu K $\alpha$  radiation (Fig. 2). Only the annealed sample presented a diffraction peak at  $2\theta = 86.6^\circ$  indicating the formation of the Ni-InGaAs phase, having the same diffraction angle found in Ref. 3.

Schottky diodes were fabricated after the residual Ni was selectively etched by concentrated HCl (37%). As a reference, Ti/Pt/Au (20/20/200 nm), Pt/Ti/Pt/Au (6/20/20/200 nm), and Pd/Ti/Pd/Au (6/20/20/200 nm) diodes on n-In<sub>0.53</sub>Ga<sub>0.47</sub>As

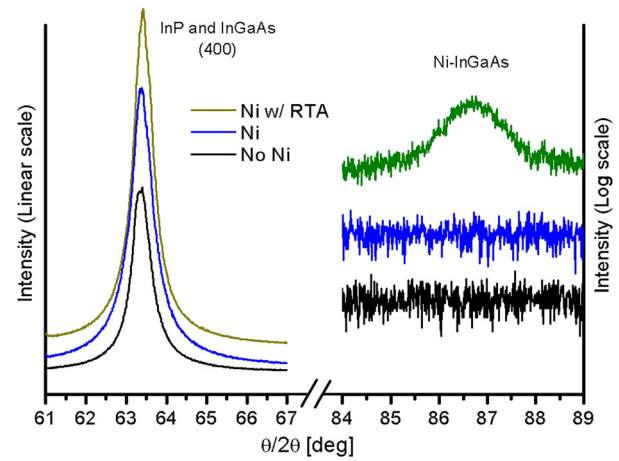


FIG. 2. X-ray diffraction of Ni-InGaAs alloy (after RTA) on InGaAs compared to bare InGaAs and InGaAs with unannealed Ni.

were fabricated. The metallic contact stack deposited on top of the Ni-InGaAs alloyed layer was Pt/Ti/Pt/Au (6/20/20/200 nm). All the samples were prepared using the same wafer, a 500 nm thick unintentionally n-type ( $\sim 1 \times 10^{16} \text{ cm}^{-3}$  Si) In<sub>0.53</sub>Ga<sub>0.47</sub>As layer lattice matched to n-InP (100) substrate grown by metal organic molecular beam epitaxy system.<sup>8</sup> Metal contacts having an area of 1000  $\mu\text{m}^2$  were patterned using photolithography and e-beam deposition. The sample was then etched for 30 s in H<sub>2</sub>SO<sub>4</sub>:H<sub>2</sub>O<sub>2</sub>:H<sub>2</sub>O 1:8:600 solution to create the diode mesa structure using the metal contacts as mask. Contact pads for wire bonding were deposited on a Si<sub>3</sub>N<sub>4</sub> layer that was deposited by plasma enhanced chemical vapor deposition system. The ohmic backside contact metals were Ti/Au 20/200 nm. Schematic illustration of the fabricated Ni-InGaAs Schottky diodes and the corresponding energy band diagram are shown in Fig. 3. Current voltage measurements were carried out by an HP 4155 A semiconductor parameter analyzer at different temperatures, ranging between 80 and 300 K for all diodes. The diodes were cooled by liquid N<sub>2</sub>, and the accuracy of the temperature measurement was better than  $\pm 1$  K.

The I-V characteristics of the Ni-InGaAs Schottky diode in the temperature range of 80–300 K are shown in Fig. 4. The corresponding logarithmic plots of  $I/[1 - \exp(-qV/k_B T)]$  as function of applied voltage are shown in Fig. 5. Note the linear nature of the plots, as long as the voltage drop across the serial resistance is small enough.

The plots shown in Fig. 5 allowed a very reliable extraction of the ideality factor and the saturation current at all temperatures. The temperature dependence of the ideality

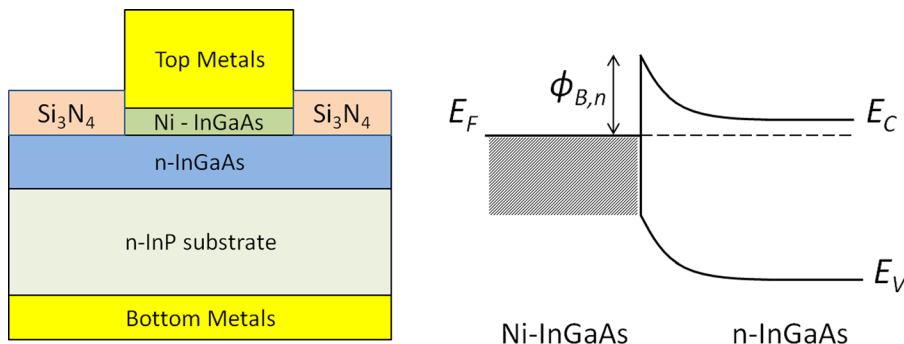


FIG. 3. Schematic illustration of the cross-section of Ni-InGaAs Schottky diodes (LHS) and the corresponding energy band diagram (RHS)

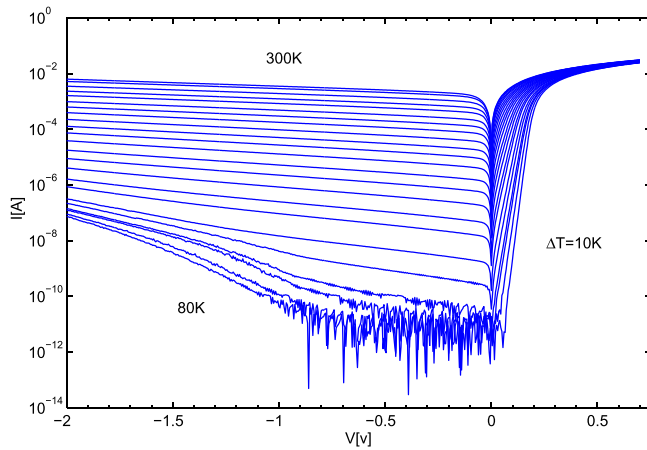


FIG. 4. Current-voltage curves of Ni-InGaAs/n-InGaAs Schottky diodes in the temperature range of 80–300 K

factor of the Ni-InGaAs diode is shown in Fig. 6 and compared to that of metallic diodes. Its value varies only slightly with temperature and is very close to the theoretical value of 1.01–1.02 calculated according to the expressions given in Ref. 4. The I-V curves of the metal diodes are not shown here. They were less ideal, and more care was needed to extract the ideality factor from linear section of the plots. The value of the metal diode ideality factors is substantially larger than those of the Ni-InGaAs diodes.

Fig. 7 presents the Richardson plots of the diodes. Note the perfectly linear dependence across the temperature range of 80–300 K of the Ni-InGaAs diodes, which allowed an accurate extraction of the energy barrier of  $0.239 \pm 0.01$  eV. By contrast, the Richardson plots of the metal diodes were linear only across limited temperature ranges, indicating that non-ideal transport mechanisms related to the interface take place. The measured parameters of the various Schottky diodes are given in Table I. For the metal diodes, the parameters were obtained from the linear section of the plot at the upper temperature range. The SBH obtained for the Ni-

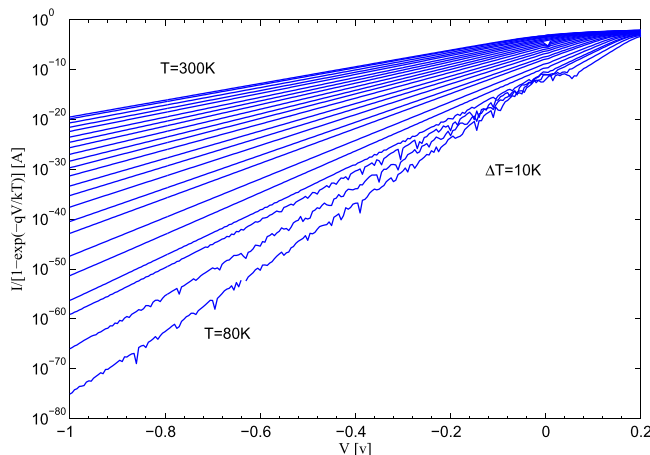


FIG. 5. Logarithmic plots of  $I/[1 - \exp(-qV/k_B T)]$  versus applied voltage for Ni-InGaAs/n-InGaAs diodes at different temperatures. The linear nature of the plots is an indication that the diodes are nearly ideal (except for the series resistance).

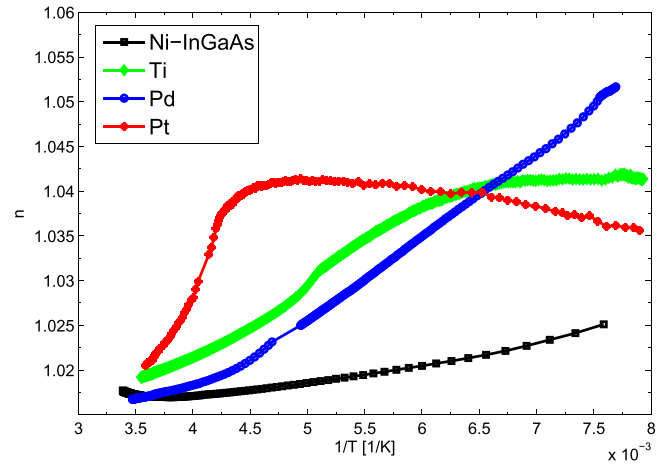


FIG. 6. Temperature dependencies of the ideality factor of the Ni-InGaAs diode and of metal diodes. The ideality factor of the Ni-InGaAs diode is close to the theoretical value of about 1.01–1.02.

InGaAs Schottky diodes is substantially higher than the values that were previously reported.<sup>2,3</sup> However, due to the perfect Richardson plot, we believe that our result is highly reliable although the HRTEM and x-ray data confirm that the Ni-InGaAs alloy is of the same phase as reported in Ref. 3. The barrier height of the Ti/InGaAs diode is similar to previously reported values<sup>9,10</sup> as well as the Pt/InGaAs SBH.<sup>9–11</sup>

In conclusion, we have found that the Ni-InGaAs Schottky diodes exhibit nearly ideal current-voltage curves, enabling an accurate extraction of the Schottky barrier height. The ideal nature of the I-V plots indicates that their interface is oxide free and clean. This “silicide like” metallization method may therefore be useful for obtaining better ohmic contacts. However, the energy barrier between Ni-InGaAs and InGaAs is larger than previously reported, indicating that ultra low contact resistance to n-type InGaAs values will be more difficult to obtain than expected. The relatively large barrier may also limit the performance of transistors having Ni-InGaAs drain and source.

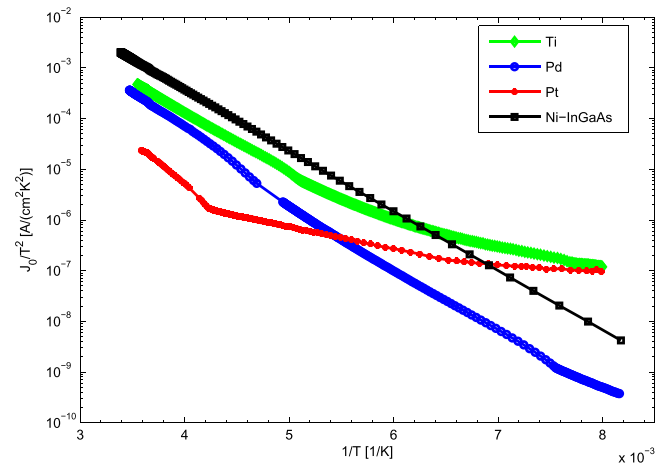


FIG. 7. Richardson plots of the Ni-InGaAs diode and of metal diodes. Note the linear behavior of the Ni-InGaAs curve across the 80–300 K temperature range. The plots of the metal diodes are linear at high temperatures only.

TABLE I. Summary of Schottky diodes parameters for different metallization.

Metallization	SBH (eV)	n
Ni-InGaAs alloy	$0.239 \pm 0.01$	1.01-1.02
Ti/Pt/Au	0.24	1.02-1.04
Pt/Ti/Pt/Au	0.32	1.02-1.04
Pd/Ti/Pd/Au	0.29	1.01-1.05

We thank Guy Cohen of IBM Yorktown Heights Research Center for suggesting our research of the Ni-InGaAs material system and for critical reading of the manuscript, Yaron Kauffmann for the TEM analysis, and Gil Bachar for assistance in the cryogenic measurements.

- <sup>1</sup>L. Czornomaz, M. El Kazzi, M. Hopstaken, D. Caimi, P. Mächler, C. Rosset, M. Bjoerk, C. Marchiori, H. Siegart, and J. Fompeyrine, *Solid-State Electron.* **74**, 71 (2012).
- <sup>2</sup>J. Pan, Z. Zhang, X. Zhang, H. Guo, X. Gong, and Y. C. Yeo, *Appl. Phys. Lett.* **99**, 012105 (2011).
- <sup>3</sup>S. H. Kim, M. Yokoyama, N. Taoka, R. Iida, S. Lee, R. Nakane, Y. Urabe, N. Miyata, T. Yasuda, and H. Yamada, *Appl. Phys. Express* **4**, 024201 (2011).
- <sup>4</sup>E. H. Rhoderick and R. H. Williams, *Metal-Semiconductor Contacts* (Clarendon Press, Oxford, 1988), pp. 89–129.
- <sup>5</sup>J. Werner, A. F. J. Levi, R. T. Tung, M. Anzlowar, and M. Pinto, *Phys. Rev. Lett.* **60**, 53 (1988).
- <sup>6</sup>M. Eizenberg, M. Heiblum, M. I. Nathan, N. Braslau, and P. M. Mooney, *J. Appl. Phys.* **61**, 1516 (1987).
- <sup>7</sup>S. M. Sze and K. K. Ng, *Physics Semiconductor Devices*, 3rd ed. (Wiley-Blackwell, NJ, 2007), pp. 170–181.
- <sup>8</sup>R. A. Hamm, D. Ritter, and H. Temkin, *J. Vac. Sci. Technol. A* **12**, 2790 (1994).
- <sup>9</sup>N. Shamir, B. Sheinman, D. Ritter, and D. Gershoni, *Solid-State Electron.* **45**, 475 (2001).
- <sup>10</sup>L. Malacký, P. Kordos, and J. Novak, *Solid-State Electron.* **33**, 273 (1990).
- <sup>11</sup>H. T. Wang, S. T. Chou, L. B. Chang, T. W. Wang, and H. C. Tang, *Appl. Phys. Lett.* **70**, 2571 (1997).